Energy Optimization of Methanol Production using CO_2 from Natural Gas Sweetening via Reactor Heat Recovery, Compressor Integration, and Cooling Water Reuse

Farrel Dzakwan Aghiffary*, Jaguar Mulia Perdana, Theona Melinda Thomson, Dania Alya Karima, Alma Camila Nathania, Renny Gustiara Rahim, Cahya Kamila Ramadhani Putri

Department of Chemical Engineering, Faculty of Engineering, Diponegoro University, Semarang 50275, Indonesia

**Corresponding Author. E-mail: farreldzakwan.ldtk1@gmail.com (Farrel Dzakwan Alghiffary)*

Telp: +625945193411

Abstract

Methanol production via CO_2 hydrogenation is an efficient alternative for supporting energy sustainability and reducing carbon emissions; however, conventional processes still face limitations in energy efficiency and resource utilization. This study aims to optimize the methanol production process through the integration of heat recovery, compressor energy utilization, and water recycling. Simulations were conducted using Aspen HYSYS by comparing baseline process conditions with modified process conditions under the same operating conditions. The results show that integrating heat from the reactor effluent and the cooling unit reduces external energy requirements, while the water recycling system successfully reduces fresh water usage by up to 100%. Additionally, heating energy requirements decreased by 27.21%, and compressor energy needs were fully met through internal energy recovery. From an economic perspective, significant operational cost savings were achieved, particularly in steam consumption, without compromising product quality, as methanol purity remained at 97.91%. Overall, the integration of mass and energy in this process has proven capable of improving efficiency, reducing costs, and supporting the sustainability of CO_2 -based methanol production.

Keywords: Methanol production; CO_2 hydrogenation; Heat integration;

Energy optimization; Water recycling

1. Introduction

Natural gas is one of the dominant energy resources worldwide, with demand projected to increase by approximately fifteen percent by 2025 [1]. It primarily consists of methane, along with smaller amounts of ethane, propane, heavier hydrocarbons, and impurities such as N_2, CO_2, H_2S, water vapor, and mercaptans. Among these, CO_2 and H_2S, commonly referred to as acid gases, must be removed to prevent corrosion, reduce environmental and health impacts, and improve the calorific value of the gas [2]. This purification step, known as natural gas sweetening, is essential in gas processing to meet safety standards, regulatory requirements, and product specifications. The most widely applied method for acid gas removal is absorption–desorption using aqueous alkanolamine solvents due to its cost effectiveness, high chemical reactivity, and adaptability to varying feed compositions [3]. However, this process is energy intensive, particularly during solvent regeneration for high acid-gas streams. In addition, the separated acid gases pose environmental challenges, prompting mitigation strategies such as carbon capture and sulfur recovery, as well as alternative utilization routes converting them into value added products like syngas for methanol production [4].

Methanol is a versatile chemical that can be utilized as a fuel substitute or additive, either in fuel cells or through direct combustion, as well as a feedstock for producing base chemicals such as formaldehyde and liquid fuels including gasoline, oxymethylene ethers, and jet fuel, in addition to its role as a solvent [5]. Reflecting its broad applicability, the global methanol market is projected to grow from 115.92 million tons in 2025 to 143.74 million tons by 2031, with a compound annual growth rate of 3.65% [6]. In conventional processes, methanol is produced from syngas through CO and CO_2 hydrogenation accompanied by the reverse water gas shift reaction, using $CuO/ZnO/Al_2O_3$ as the catalyst [7].

Existing studies on CO_2 utilization for methanol production have primarily focused on catalyst development, thermodynamic limitations, and reaction kinetics to improve conversion and selectivity [8]. In parallel, process design and optimization

studies have investigated methanol synthesis through strategies such as heat integration, recycle configuration, and operating condition optimization to enhance energy efficiency [9]. However, most of these approaches are applied individually and are limited to partial system boundaries, particularly without simultaneous consideration of reactor heat recovery, compressor work integration, and cooling utility optimization within a unified framework. As a result, the potential for comprehensive energy optimization across interconnected process units remains insufficiently explored.

To address this gap, this study develops an integrated process simulation for methanol production using CO_2 derived from natural gas sweetening, with a focus on system-level energy optimization. A unified process configuration is employed to evaluate the combined effects of reactor heat recovery, compressor integration, and cooling water reuse on overall energy performance. This framework enables systematic reduction of energy demand through coordinated interaction between process units, rather than isolated optimization of individual subsystems. Accordingly, the objective of this study is to assess the impact of integrated energy optimization on the performance and efficiency of CO_2-based methanol production systems.

2. Methods

2.1. Methanol Production Process

The CO_2 utilized for methanol synthesis in this study is sourced from the natural gas sweetening process. The feed gas composition, as shown in Table 1, consists predominantly of methane along with light hydrocarbons, acid gases (CO_2 and H_2S), and minor impurities such as nitrogen and water. As illustrated in Figure 1, the process was simulated using Aspen HYSYS to represent the absorption–regeneration system. The gas stream is introduced into an absorber column, where it is contacted counter-currently with an aqueous solution of methyldiethanolamine (MDEA) at 20 wt% diluted in 80 wt% water [10].

MDEA is selected due to its high selectivity toward acid gases and its relatively low regeneration energy requirement compared to primary and secondary amines,

making it suitable for energy-efficient gas sweetening processes [11]. Within the absorber, the amine selectively removes acid gases, primarily CO_2 and H_2S, producing a sweetened natural gas stream with reduced impurity levels. The resulting rich MDEA solution is then sent to a regeneration unit, where it is heated to release the absorbed gases. During this step, CO_2, H_2S, and trace amounts of co-absorbed components such as nitrogen and light hydrocarbons are desorbed. The recovered CO_2 stream is subsequently separated and directed as a feedstock for methanol synthesis, establishing an integrated pathway between natural gas sweetening and CO_2 utilization [11].

Methanol is produced via the catalytic hydrogenation of carbon dioxide, a reaction system increasingly recognized for its relevance to carbon capture and utilization (CCU) and sustainable fuels production. Industrial methanol synthesis operates in the gas phase within high-pressure fixed-bed reactors, typically employing metal-oxide catalysts capable of activating CO_2 under moderate temperatures and elevated hydrogen partial pressures [12]. Modern process designs emphasize operation between 220-280°C, where a balance is achieved between kinetic activity and the thermodynamic constraints associated with CO_2 conversion.

Under these operating conditions, CO_2 hydrogenation proceeds through a network of parallel and consecutive reactions. The primary and desired pathway leads to methanol formation, while the reverse water–gas shift (RWGS) reaction can also occur, producing CO as an intermediate species. The generated CO may subsequently undergo hydrogenation to methanol, contributing to overall methanol formation. These reactions can be expressed as follows [12].

CO_2 hydrogenation (methanol synthesis):

$$CO_2 + 3H_2 \rightarrow CH_3OH + H_2O \quad \Delta H^0_{298K} = -49.5 \text{ kJ/mol} \tag{1}$$

Side reaction (reverse water-gas shift, RWGS)

$$CO_2 + H_2 \rightarrow CO + H_2O \quad \Delta H^0_{298K} = +41.2 \text{ kJ/mol} \tag{2}$$

Side reaction (CO_2 hydrogenation)

$$CO_2 + 2H_2 \rightarrow CH_4 + 2H_2O \quad \Delta G^0_{298K} = -130.8 \text{ kJ/mol} \tag{3}$$

Over a particle bed of a zirconia-based catalyst, reactor performance was represented based on experimental data reported by Yang *et al.* [13] at an operating pressure of 50 bar and a temperature of 250 °C. Under these conditions, a CO_2

conversion of 15% was assumed for the CO_2 hydrogenation reaction (Eq. 1), 10% for the RWGS reaction (Eq. 2), and 50% for the CO hydrogenation to methanol reaction (Eq. 3). In each simulation run, the molar ratio of H_2 to CO_2 at the reactor inlet was maintained at a constant value of 3:1 in accordance with the stoichiometric requirement of methanol synthesis.

The conceptual development of CO_2-to-methanol process flowsheets has expanded rapidly in recent years due to advances in catalyst technology and the integration of green hydrogen. Recent studies have focused on optimizing process configurations to improve thermal management, energy integration, and CO_2 conversion efficiency, including the implementation of reactor–separator loop designs and hybrid catalytic-electrolytic systems. Similar to conventional syngas-based methanol plants, CO_2-based systems typically incorporate recycle loops to enhance single-pass conversion, given the thermodynamic limitations associated with reaction (1).

Industrial reactor configurations generally operate at pressures between 20 and 55 bar to overcome these equilibrium constraints. Elevated pressure promotes methanol formation because the main synthesis reaction results in a net reduction in gas-phase moles. In contrast, reaction temperatures are intentionally limited to prevent the equilibrium from shifting toward the reverse water–gas shift (RWGS) pathway (reaction 2). Catalyst thermal stability and the inhibitory effect of water further restrict the upper temperature limit, leading most systems to avoid operation above 300°C to preserve both activity and selectivity. As indicated by the kinetic analysis, the RWGS reaction exhibits a lower activation energy compared to methanol synthesis, causing CO formation to dominate at higher temperatures. The subsequent hydrogenation of CO provides an additional route for methanol formation under suitable operating conditions [12]. Consequently, optimal selectivity toward methanol is achieved by maintaining moderate temperatures, ensuring sufficient hydrogen availability, and minimizing the accumulation of water within the reaction environment.

The $Cu/ZnO/Al_2O_3$ catalyst system, which remains the industrial benchmark for methanol synthesis, is widely recognized for its high activity and stability under conventional operating conditions. In this catalyst, Cu sites serve as the primary

active phase for CO and CO_2 hydrogenation, while ZnO and Al_2O_3 function as structural and electronic promoters that enhance metal dispersion, thermal stability, and resistance to sintering. Despite its proven industrial robustness, the $Cu/ZnO/Al_2O_3$ catalyst system faces inherent challenges under CO_2-rich feeds, particularly due to water formation and the promotion of the reverse water–gas shift reaction, which can reduce methanol selectivity and accelerate catalyst deactivation. Nevertheless, its extensive industrial utilization and well-established kinetic behavior make $Cu/ZnO/Al_2O_3$ a suitable benchmark catalyst for process modeling and reactor level optimization studies.

2.2. Thermodynamic and Reaction Pathway Analysis

The thermodynamic analysis of the CO_2 conversion system presented in the study relies on the standard Gibbs free energy of reaction at 298 K ($\Delta G^{\circ}_{r,\,298K}$). Data $\Delta G^{\circ}_{f\,298K}$ of each component to determine ΔG_r at 298K [14]. [4] The value of $\Delta G^{\circ}_{r\,298K}$ for the reaction is obtained by:

$$\Delta G^{\circ}_{r\,298K} = \sum \Delta G^{\circ}_{f\,298K\,product} - \sum \Delta G^{\circ}_{f\,298K\,reactant} \quad (4)$$

$$\Delta G^{\circ}_{r\,298K} = (\Delta G^{\circ}_{f\,298K\,CH_3OH} + \Delta G^{\circ}_{f\,298K\,H_2O}) - (\Delta G^{\circ}_{f\,298K\,CO_2} + \Delta G^{\circ}_{f\,298K\,H_2})$$

$$\Delta G^{\circ}_{r\,298K} = [(-162.2)+(-228.6)] - [(-394.4)+3(0)]\,kJ/mol$$

$$\Delta G^{\circ}_{r\,298K} = +3.6\ kJ/mol$$

The value of $\Delta H^{\circ}_{r\,298K}$ for the reaction is obtained by:

$$\Delta H^{\circ}_{r\,298K} = \sum \Delta H^{\circ}_{f\,298K\,product} - \sum \Delta H^{\circ}_{f\,298K\,reactant} \quad (5)$$

$$\Delta H^{\circ}_{r\,298K} = (\Delta H^{\circ}_{r\,298K\,CH_3OH} + \Delta H^{\circ}_{r\,298K\,H_2O}) - (\Delta H^{\circ}_{r\,298K\,CO_2} + \Delta H^{\circ}_{r\,298K\,H_2})$$

$$\Delta H^{\circ}_{r\,298K} = [(-200.9)+(-241.8)] - [(-393.5)+3(0)]\,kJ/mol$$

$$\Delta H^{\circ}_{r\,298K} = -49.2\ kJ/mol$$

These data indicate that, under standard conditions, certain pathways exhibit favorable thermodynamic tendencies while others remain non-spontaneous. The equilibrium constant at 298 K is determined from these values through the standard thermodynamic relationship:

$$\ln K_{298} = -\frac{\Delta G^{\circ}_{r,\,298K}}{RT} \quad (6)$$

For the dominant route, the evaluation yields:

$$\ln K_{298} = \frac{-\left(+3600\ \frac{J}{mol}\right)}{8.314\ \frac{J}{mol.K} \times 298\ K}$$

$$\ln K_{298} = -1.45$$

$$K_{298} = 0.23 \quad (7)$$

The resulting value suggests that, at standard temperature, The reaction exhibits limited thermodynamic favorability under standard conditions and remains close to equilibrium. To evaluate the effect of temperature on equilibrium, the integrated van't Hoff equation is applied:

$$\ln\left(\frac{K_T}{K_{298}}\right) = \frac{\Delta H_r^\circ}{R}\left(\frac{1}{298} - \frac{1}{T}\right) \quad (8)$$

The standard enthalpy change used is ΔH_r° = -49.2 kJ/mol [12]. Substitution into Eq. (2) at a representative operating temperature of 523 K gives:

$$\ln\left(\frac{K_{523}}{0.23}\right) = \frac{-49200\ J/mol}{8.314\ J/(mol \cdot K)}\left(\frac{1}{298} - \frac{1}{523}\right) \quad (9)$$

$$K_{523} = 4.4 \times 10^{-5} \quad (10)$$

This marked reduction in the equilibrium constant at elevated temperature highlights the strong thermodynamic limitation imposed on the system at industrially relevant conditions. As such, elevated pressure is required to counteract equilibrium constraints and sustain appreciable conversion levels [15].

Despite the thermodynamic tendencies indicated by the equilibrium analysis, the actual methanol formation is also influenced by reaction pathways under industrial conditions. Experimental data over a zirconia-based catalyst bed at 50 bar and 250°C indicate that CO_2 hydrogenation to methanol achieves a relatively low conversion of 15%, while the reverse water-gas shift reaction reaches 10%, and CO hydrogenation to methanol shows a significantly higher conversion of 50% [16]. This disparity suggests that the indirect pathway via CO plays a dominant role in methanol formation. Consequently, maintaining an appropriate hydrogen supply becomes essential to drive the reaction toward methanol production. Therefore, an inlet H_2 to CO_2 molar ratio of 3 to 1 is commonly employed to ensure sufficient hydrogen availability and to enhance overall conversion.

2.3. Process Simulator Tool

The methanol production process through CO_2 hydrogenation was simulated

using Aspen HYSYS V15. This simulation enables integrated modeling of chemical reactions, thermodynamic equilibrium, and unit operations within a complex process system. The selection of fluid packages is a crucial step, as it determines the accuracy of phase equilibrium predictions, thermodynamic properties, and physical characteristics of mixtures. In this simulation, three fluid packages were applied according to the characteristics of each process stage.

Acid Gas Treatment employed Methyl diethanolamine (MDEA), chosen because it is tertiary alkanolamine and the most used agent in acid gas processing. As a tertiary amine, MDEA is highly selective toward H_2S, a component that must be completely removed in the process [15]. Peng-Robinson EOS (PR EOS) was used in the compression stage and CO_2 hydrogenation reactor due to its accuracy in predicting the thermodynamic properties of light gas mixtures under high pressure. PR EOS supports the estimation of phase equilibrium, mixture energy, and reaction enthalpy under conditions of 50-100 bar and 200-300°C [17]. The final model, NRTL (Non-Random Two Liquids), was applied to methanol-water distillation because this binary system is highly non-ideal due to hydrogen bonding. Based on activity coefficients, NRTL is more accurate than PR EOS in predicting vapor-liquid equilibrium, relative volatility, and dew points of the mixture [18].

2.4 Mass & Energy Optimization Method

Mass and energy optimization in chemical process systems can be effectively achieved through the integration of recycle streams and heat recovery strategies within the process flowsheet. In the modified configuration, process streams that still contain valuable components or thermal energy are not discharged but instead redirected for reuse [19]. From a mass perspective, recycle streams are introduced to recover unutilized materials and reduce the demand for fresh feed or utility streams. For instance, process water or working fluids that have undergone temperature changes can still be reused as modified streams to replace unmodified utility water, thereby minimizing fresh water consumption. The effectiveness of this mass optimization approach can be evaluated using the following expression:

$$\text{Water Saving (\%)} = \frac{m_{\text{unmodified}} - m_{\text{modified}}}{m_{\text{unmodified}}} \quad (11)$$

This approach is consistent with recent developments in process integration,

where closed-loop systems are designed to maximize internal resource utilization and reduce waste generation. Studies have shown that integrating water reuse networks with process systems can significantly reduce freshwater demand and operational costs while improving environmental sustainability [17]. By implementing such recycle strategies, the process achieves higher material efficiency, reduces dependency on external utilities, and enhances overall process performance. In addition to mass optimization, energy efficiency is improved through the recovery and reutilization of heat from high-temperature process streams. Thermal energy from reactor effluent or high-pressure steam (HPS) conditions can be transferred via heat exchangers to preheat incoming streams or supply energy to other process units, thereby reducing the need for external heating utilities. Although the total heat duty required by the system remains constant, the substitution of external utilities with internally recovered heat leads to significant cost savings. The reduction in utility energy consumption can be quantified as:

$$\text{Energy Saving (\%)} = \frac{Q_{unmodified} - Q_{modified}}{Q_{unmodified}} \quad (12)$$

This method reflects the principles of heat integration, where energy is conserved by matching hot and cold streams within the process. Previous studies have demonstrated that heat recovery systems can substantially reduce energy consumption and operating costs in industrial applications [19]. For example, the implementation of waste heat recovery technologies has been reported to achieve energy savings of up to 16.1% compared to conventional systems, depending on process configuration. In addition, heat recovery efficiency can reach values above 60%, indicating a significant improvement in thermal utilization. Furthermore, modified configurations such as multi-stage heat recovery systems have been shown to enhance net heat recovery by more than 20% compared to baseline designs [20]. These findings clearly confirm that modified processes incorporating heat integration are more energy efficient than unmodified systems. Therefore, the combined implementation of mass recycle and heat recovery provides a comprehensive optimization strategy that enhances both economic efficiency and sustainability in chemical process design.

3. Results and Discussion

3.1. Comparison Between Basic and Modified Processes

The simulations of both the baseline and modified methanol production processes were carried out using Aspen HYSYS to evaluate the impact of mass and energy optimization strategies. In the baseline configuration, process heating is primarily supplied by external utilities, particularly high-pressure steam (HPS), to achieve the desired reactor inlet temperature. The reactor operates at 250°C and 50 bar, which are within the typical industrial range for methanol synthesis, producing a final methanol purity of 97.91% after downstream purification. However, in this conventional configuration, the heat released from exothermic reactions and cooling processes is not effectively utilized and is instead rejected to the environment, resulting in inefficient energy utilization. Additionally, utility water is consumed directly without internal reuse, leading to higher overall resource demand. The overall structure of the unmodified process is presented in Figure 2.

In contrast, the modified process, as illustrated in Figure 3, introduces an integrated heat and mass recovery network designed to enhance overall process efficiency. Several key heat integration strategies were implemented across major equipment units. First, Heat Exchanger (E-100) is optimized by utilizing the cooling water outlet from Heat Exchanger (E-101) as a secondary thermal resource. This cascading heat utilization reduces the requirement for fresh cooling water in E-100, thereby significantly decreasing utility water consumption. Second, Heat Exchanger (E-102) recovers heat released from the reactor conversion section and redirects it for feed preheating, which reduces dependence on external heating utilities such as high-pressure steam. Third, Compressor (K-102) partially utilizes recovered energy from Cooler (E-105), where waste thermal energy is converted into useful process energy, improving overall system efficiency.

3.2. Mass & Energy Efficiency

A significant improvement in mass efficiency is observed through the implementation of a water recycle system in heat exchanger E-100. As indicated in Table 2, the total process water requirement remains unchanged at 1213 kg/h in both configurations; however, the source of this water differs fundamentally. In the

baseline case, the entire demand is supplied by fresh utility water, whereas in the modified process, this requirement is completely fulfilled by recycled water from the outlet of heat exchanger E-101. This results in a 100% reduction in fresh water consumption, demonstrating the effectiveness of internal stream reuse in minimizing external resource dependency. Such a closed-loop approach reflects an optimized mass integration strategy, where process streams are systematically reused to enhance overall efficiency without altering operational demand.

Energy optimization is further achieved through the integration of heat recovery in heat exchanger E-102. As shown in Table 3, both configurations operate under identical thermodynamic conditions, with a temperature of 250°C, a pressure of 55 bar, and a fully vapor-phase stream. Despite these similarities, a notable reduction in mass flow rate is observed, decreasing from 4786.90 kg/h in the unmodified process to 3484.10 kg/h in the modified configuration, corresponding to a reduction of 27.21%. This reduction indicates that part of the heating requirement is satisfied by internally recovered thermal energy, thereby reducing the reliance on external heating utilities. The ability to maintain the same operating conditions while lowering the required input highlights the effectiveness of heat integration in improving energy utilization within the system [21].

Further enhancement is evident in the energy supply strategy of compressor K-102. According to Table 4, the required heat duty remains constant at 204,156.84 kJ/h, indicating that the operational demand of the unit is unchanged between the two configurations. However, the origin of this energy undergoes a complete transformation. In the baseline process, the compressor relies entirely on external utilities, whereas in the modified configuration, the required energy is fully supplied by recovered heat from unit E-105. This represents a 100% substitution of external energy, illustrating a successful transition from utility-dependent operation to internally sustained energy utilization. Such a shift not only improves process efficiency but also reduces operational reliance on external energy sources.

Taken together, the integration of water recycling, heat recovery, and energy source substitution demonstrates a comprehensive improvement in both mass and energy efficiency. The elimination of fresh water usage, reduction in heating demand, and complete replacement of external energy in the compressor collectively indicate

a more sustainable and resource-efficient process design. Importantly, these enhancements are achieved without altering operating conditions or compromising process performance. The stability of the system is further confirmed by the final product specification, where methanol purity is maintained at 97.91%, indicating that the applied optimization strategies do not adversely affect product quality while significantly improving overall process efficiency [22].

3.3. Cost Efficiency Analysis Based on Mass and Energy Optimization

Table 5 presents the estimation of steam production cost using the boiler cost correlation reported in [21], which is derived from an overall energy balance around the boiler. The fuel cost component for steam generation is calculated using:

$$C_F = a_F \times \frac{H_s - h_w}{1000\eta_B} \quad (13)$$

where a_F is the natural gas price (2.6702 $/MMBtu from [23]), Hs is the enthalpy of saturated steam, hw is the enthalpy of boiler feedwater, and ηB is the boiler efficiency. Based on the given thermodynamic data and a boiler efficiency of 0.8, the calculated fuel cost is 8.7 $/1000 lb of steam. The total steam production cost is then estimated using [23]:

$$C_G = C_F(1+0.3) \quad (14)$$

which accounts for additional operating and maintenance expenses equal to 30% of the fuel cost. Using this approach, the final steam cost is obtained as 11.31 $/1000 lb.

The impact of this steam cost is further reflected in the economic performance of the heat exchanger network, particularly in Heat Exchanger E-100, which utilizes high-pressure steam (HPS). As shown in Table 6, the modified process significantly reduces the steam consumption from 4786.90 kg/h to 3484.10 kg/h, corresponding to a reduction of approximately 27.2%. This reduction directly lowers the operating cost from 1,002,815.92 $/year to 729,890.85 $/year, resulting in an annual cost saving of 272,925.08 $/year. This demonstrates that mass and energy optimization effectively minimizes utility demand, especially for high-cost utilities such as steam.

In addition to steam, cooling water requirements are also evaluated, as shown in Table 7 for Heat Exchanger E-102. The cooling water flowrate is relatively small at 1213 kg/h, with a unit cost of 0.0000373 $/kg [24] , resulting in a negligible operating cost of only 380.06 $/year. This indicates that, compared to steam, cooling

water does not significantly contribute to the overall utility cost and therefore has a minimal impact on economic optimization.

Lastly, the electricity consumption associated with Compressor K-102 is presented in Table 8. The compressor requires a power input of 56.71 kWh, leading to an operating cost of 85,745.88 $/year at an electricity price of 0.18 $/kWh [25]. Although this cost is lower than the steam-related expenses, it still represents a considerable portion of the total utility cost and should be included in the overall economic evaluation. Overall, the results indicate that steam consumption dominates the utility cost structure; therefore, optimization strategies focusing on heat integration and steam reduction provide the most significant economic benefits. The overall utility cost savings achieved through these optimizations are summarized in Table 9.

4. Conclusion

The modification of the methanol production process successfully improves mass and energy efficiency through heat integration, water recycling, and energy recovery. The results show a 100% reduction in fresh water usage and a 27.21% decrease in heating demand in Heat Exchanger E-102, while maintaining the same operating conditions. In addition, the energy requirement of Compressor K-102 is fully supplied by recovered heat, achieving complete substitution of external energy. From an economic perspective, steam dominates the utility cost, with a value of 11.31 $/1000 lb. The reduction in steam consumption leads to a significant annual cost saving of 272,925.08 $/year, while cooling water and electricity contribute relatively minor costs. Importantly, these improvements are achieved without compromising product quality, with methanol purity remaining at 97.91%. Overall, the modified process is more efficient and sustainable, demonstrating that heat integration and resource optimization effectively reduce utility consumption and operating costs in methanol production.

CRediT Author Statement

F.D. Aghiffary: Conceptualization, Methodology, Investigation, Software,

Visualization, Writing, Review & Editing, Supervision. J.M. Perdana: Conceptualization, Methodology, Visualization, Writing, Review & Editing, Project Administration, Validation. T.M. Thomson: Conceptualization, Methodology, Formal Analysis, Resources, Validation, Writing. D.A. Karima: Conceptualization, Methodology, Investigation, Resources, Data Curation, Writing. A.C. Nathania: Conceptualization, Methodology, Investigation, Resources, Data Curation, Writing. R.G. Rahim: Data Curation, Formal Analysis, Visualization, Writing-Review & Editing. C.K.R. Putri: Data Curation, Resources, Visualization, Writing-Review & Editing.

Reference

[1] International Energy Agency. (2020). *Global gas demand in initial and revised forecasts, 2019–2025*. Retrieved April 24, 2026, from https://www.iea.org/data-and-statistics/charts/global-gas-demand-in-initial-and-revised-forecasts-2019-2025

[2] Darani, N. S., Behbahani, R. M., Shahebrahimi, Y., Asadi, A., & Mohammadi, A. H. (2021). Simulation and optimization of the acid gas absorption process by an aqueous diethanolamine solution in a natural gas sweetening unit. *ACS omega*, *6*(18), 12072-12080. https://doi.org/10.1021/acsomega.1c00744

[3] Mohajeri, M., Panahi, M., & Shahsavand, A. (2024). Optimal operation of a natural gas sweetening plant. *Computers & Chemical Engineering*, *184*, 108631. https://doi.org/10.1016/j.compchemeng.2024.108631

[4] Solis-Jacome, A., Ramírez-Márquez, C., Morales-Cabrera, M. A., & Ponce-Ortega, J. M. (2024). Methanol production from residual streams of natural gas sweetening for achieving the sustainable development goals. *Chemical Engineering and Processing - Process Intensification*, *199*, 109746. https://doi.org/10.1016/j.cep.2024.109746

[5] Lacerda de Oliveira Campos, B., John, K., Beeskow, P., Herrera Delgado, K., Pitter, S., Dahmen, N., & Sauer, J. (2022). A detailed process and techno-economic analysis of methanol synthesis from H2 and CO2 with intermediate condensation steps. *Processes*, *10*(8), 1535. https://doi.org/10.3390/pr10081535

[6] Mordor Intelligence. (2026). *Methanol market size, share, trends analysis & industry report (2031).* Retrieved April 24, 2026, from https://www.mordorintelligence.com/industry-reports/methanol-market

[7] Borisut, P., & Nuchitprasittichai, A. (2019). Methanol Production via CO2 Hydrogenation: Sensitivity Analysis and Simulation—Based Optimization. *Frontiers in Energy Research*, *7*. https://doi.org/10.3389/fenrg.2019.00081

[8] Kanuri, S., Roy, S., Chakraborty, C., Datta, S. P., Singh, S. A., & Dinda, S. (2022). An insight of CO2 hydrogenation to methanol synthesis: Thermodynamics, catalysts, operating parameters, and reaction mechanism. *International Journal of Energy Research*, *46*(5), 5503-5522. https://doi.org/10.1002/er.7562

[9] Francis, A., Ramyashree, M. S., Priya, S. S., Kumar, S. H., Sudhakar, K., Fan, W. K., & Tahir, M. (2022). Carbon dioxide hydrogenation to methanol: Process simulation and optimization studies. *International Journal of Hydrogen Energy*, *47*(86), 36418-36432. https://doi.org/10.1016/j.ijhydene.2022.08.215

[10] Machado, C. F. R., Medeiros, J. L., Araújo, O. F. Q., & Alves, R. M. B. (2014). A comparative analysis of methanol production routes: synthesis gas versus CO_2 hydrogenation. *In Proceedings of the International Conference on Industrial Engineering and Operations Management*.

[11] Francis, A., MS, R., Priya, S. S., Kumar, S. H., Sudhakar, K., Fan, W. K., & Tahir, M. (2022). Carbon dioxide hydrogenation to methanol: Process simulation and optimization studies. *International Journal of Hydrogen Energy*, *47*(86), 36418–36432. https://doi.org/10.1016/j.ijhydene.2022.08.215

[12] Abooali, D., Soleimani, R., & Rezaei-Yazdi, A. (2020). Modeling CO2 absorption in aqueous solutions of DEA, MDEA, and DEA+ MDEA based on intelligent methods. *Separation Science and Technology*, *55*(4), 697-707. https://doi.org/10.1080/01496395.2019.1575415

[13] Yang, N., Kang, F., Liu, Z., Ge, X., & Zhou, Y. (2022). An integrated CCU-plant scheme and assessment for conversion of captured CO2 into methanol. *International Journal of Low-Carbon Technologies*, *17*, 550–562. https://doi.org/10.1093/ijlct/ctac038

[14] Yaws, C. L. (2003). *Yaws' handbook of thermodynamic and physical properties of chemical compounds*. Knovel.

[15] Ren, M., Zhang, Y., Wang, X., & Qiu, H. (2022). Catalytic Hydrogenation of CO2 to methanol: a review. *Catalysts*, *12*(4), 403. https://doi.org/10.3390/catal12040403

[16] Park, N., Park, M.-J., Ha, K.-S., Lee, Y.-J., & Jun, K.-W. (2014). Modeling and analysis of a methanol synthesis process using a mixed reforming reactor: Perspective on methanol production and CO_2 utilization. Fuel. https://doi.org/10.1016/j.fuel.2014.03.068

[17] Ahmetović, E., Kravanja, Z., & Grossmann, I. E. (2022). Combined water and heat integration in process industries. *Frontiers in Chemical Engineering, 4*, 1012754. https://doi.org/10.3389/fceng.2022.1012754

[18] Valverde, J., Ferro, V., & Giroir-Fendler, A. (2022). Application of the e-NRTL model to electrolytes in mixed solvents methanol-, ethanol- water, and PEG-water. *Fluid Phase Equilibria*, *560*, 113516. https://doi.org/10.1016/j.fluid.2022.113516

[19] Lee, J.-Y., & Chen, P.-Y. (2023). Optimization of heat recovery networks for energy savings in industrial processes. *Processes, 11*(2), 1-9. 10.21608/eajast.2022.146577.1011

[20] Liu, C., Ma, H., Liu, S., Zhang, H., & Ma, D. (2024). Heat recovery technology and energy-saving effect analysis applied to cleanroom exhaust waste heat characteristics. Energy & Buildings, 306, 113935. https://doi.org/10.1016/j.enbuild.2024.113935

[21] Ribeiro, J. M., Dias, D. F. C., Nika, E., Delpech, B., Katsou, E., & Jouhara, H. (2025). Circularity assessment of industrial heat exchanger and water treatment systems integration. *Thermal Science and Engineering Progress, 62*, 103661. https://doi.org/10.1016/j.tsep.2025.103661

[22] Hall, S. (2017). *Rules of thumb for chemical engineers*. Elsevier Science. https://doi.org/10.1016/C2016-0-00182-1

[23] Trading Economics. (2026). *Natural gas prices*. Retrieved April 11, 2026, from https://tradingeconomics.com/commodity/natural-gas

[24] Intratec. (2026). *Cooling water cost in the United States*. Retrieved April 11, 2026, from https://www.intratec.us/solutions/industry-economics-worldwide/utility/cooling-water-cost-united-states

[25] World Population Review. (2026). *Cost of electricity by country*. Retrieved April 11, 2026, from https://worldpopulationreview.com/country-rankings/cost-of-electricity-by-country

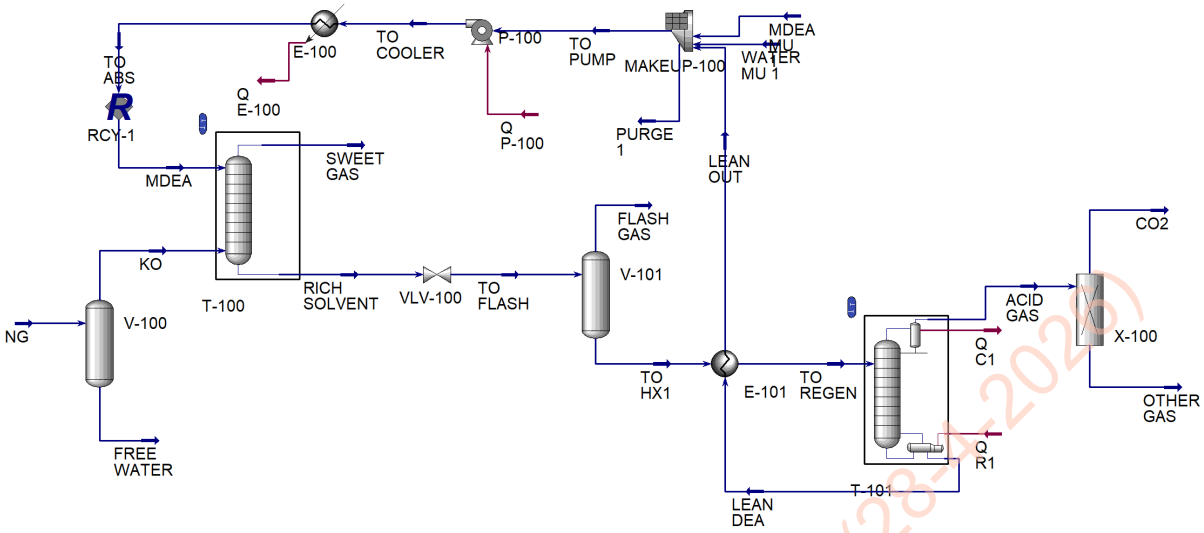

Figure 1. Simulation using Aspen HYSYS of natural gas sweetening

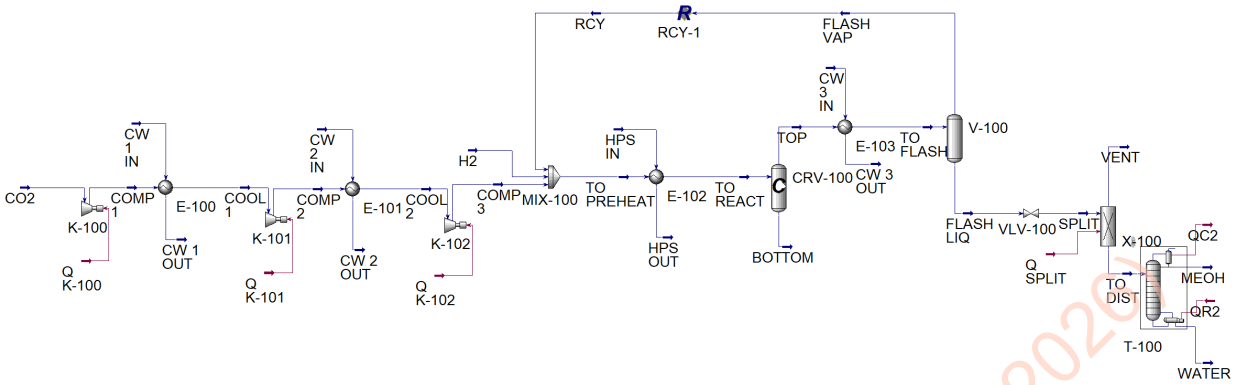

Figure 2. Methanol production using Aspen HYSYS of (basic) unmodified process

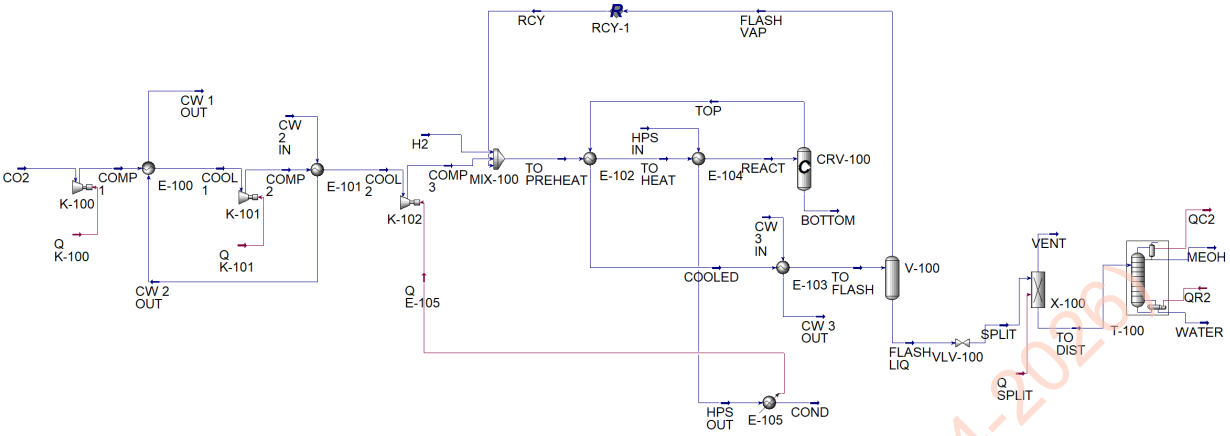

Figure 3. Methanol production using Aspen HYSYS of modified process

Table 1. Natural gas composition

Component	Mole Fraction
Methane	0.8692
Ethane	0.0393
Propane	0.0093
i-Butane	0.0026
n-Butane	0.0029
i-Pentane	0.0014
n-Pentane	0.0012
n-Hexane	0.0018
Nitrogen	0.0016
H2S	0.0172
CO2	0.0413
H2O	0.0122

Table 2. Comparison of water consumption (HPS) and savings between unmodified and modified processes (E-100)

Heat Exchanger (E-100)			
Parameter	Unmodified	Modified	Remarks
	Inlet Stream (CW-1 In)	Inlet Stream (CW-2 Out)	
Total process water requirement (kg/h)	1213	1213	Constant demand
Water (unmodified) (kg/h)	1213	0	Supplied from utilities
Recycled water (modified) (kg/h)	0	1213	From E-101 outlet
Fresh water saving (kg/h)	0	1213	Reduction in utility consumption
Saving percentage (%)	-	100%	Ideal condition (no losses considered)

Table 3. Comparison of stream properties in heat exchanger E-102

Heat Exchanger (E-102)			
Parameter	Unmodified Inlet Stream (HPS In)	Modified Inlet Stream (TOP)	Remarks
Vapor Phase Fraction	1	1	Fully vapor phase
Temperature (°C)	271,2680054	271,2680054	Target temperature achieved
Pressure (bar)	55	55	Operating pressure maintained
Molar Flow (Kmol/h)	265,7157127	193,3988731	Reduced due to heat recovery
Mass Flow (kg/h)	4786,895263	3484,100132	Lower fresh feed requirement
Saving percentage (%)	-	27.21%	Ideal condition (no losses considered)

Table 4. Comparison of energy source and heat duty in compressor K-102

Compressor (K-102)			
Parameter	Unmodified	Modified	Remarks
Heat Flow (kJ/h)	204,156.84	204,156.84	Same energy requirement
Energy Source	Utility	E-105 (Recovered Heat Duty)	Shift from external to internal source
Saving percentage (%)	-	100%	Ideal condition (no losses considered)

Table 5. Steam Cost Calculation Based on Natural Gas Fuel

Calculation of steam cost			
Fuel type		Natural Gas	
Fuel cost	aF	2,6702	$/MMBtu
Enthalpy of steam	Hs	2643,1965	Btu/lb
Enthapy of boiler feedwater	hw	36,1	
Boiler efficiency	eta	0,8	
Fuel cost	CF	8,70	$/1000lb
Steam cost	CG	11,31	$/1000lb

Table 6. Comparison of High-Pressure Steam (HPS) Cost for Heat Exchanger E-100 in Unmodified and Modified Processes

HPS cost (Heat Exchanger E-100)		
Parameter	(Unmodified)	Modified
Mass flow (kg/h)	4786,8953	3484,1001
(lb/h)	10553,285	7681,117
Price ($/h)	119,383	86,892
($/yr)	1002815,923	729890,8453
Cost saving ($/yr)	272925,0775	

Table 7. Cooling Water Cost for Heat Exchanger E-102

Cooling Water (E-102)	
Mass Flow (kg/h)	1213
Cooling water cost ($/kg)	0,0000373
Price ($/h)	0,0452
($/yr)	380,0572

Table 8. Electricity Cost for Compressor K-102

Compresor K-102	
Heat Flow (kJ/h)	204,156.84
(kwh)	56,7102
Electricity cost ($/kwh)	0,18
Price ($/h)	10,2078
($/yr)	85745,8797

Table 9. Total Utility Cost Savings from Process Integration

Total Cost Saving		
HPS saving E-100	($/yr)	272925.0775
Compresor K-102	($/yr)	85745.8797
Cooling Water E-102	($/yr)	380.0572
Total	($/yr)	359051.0143